Published

JEM

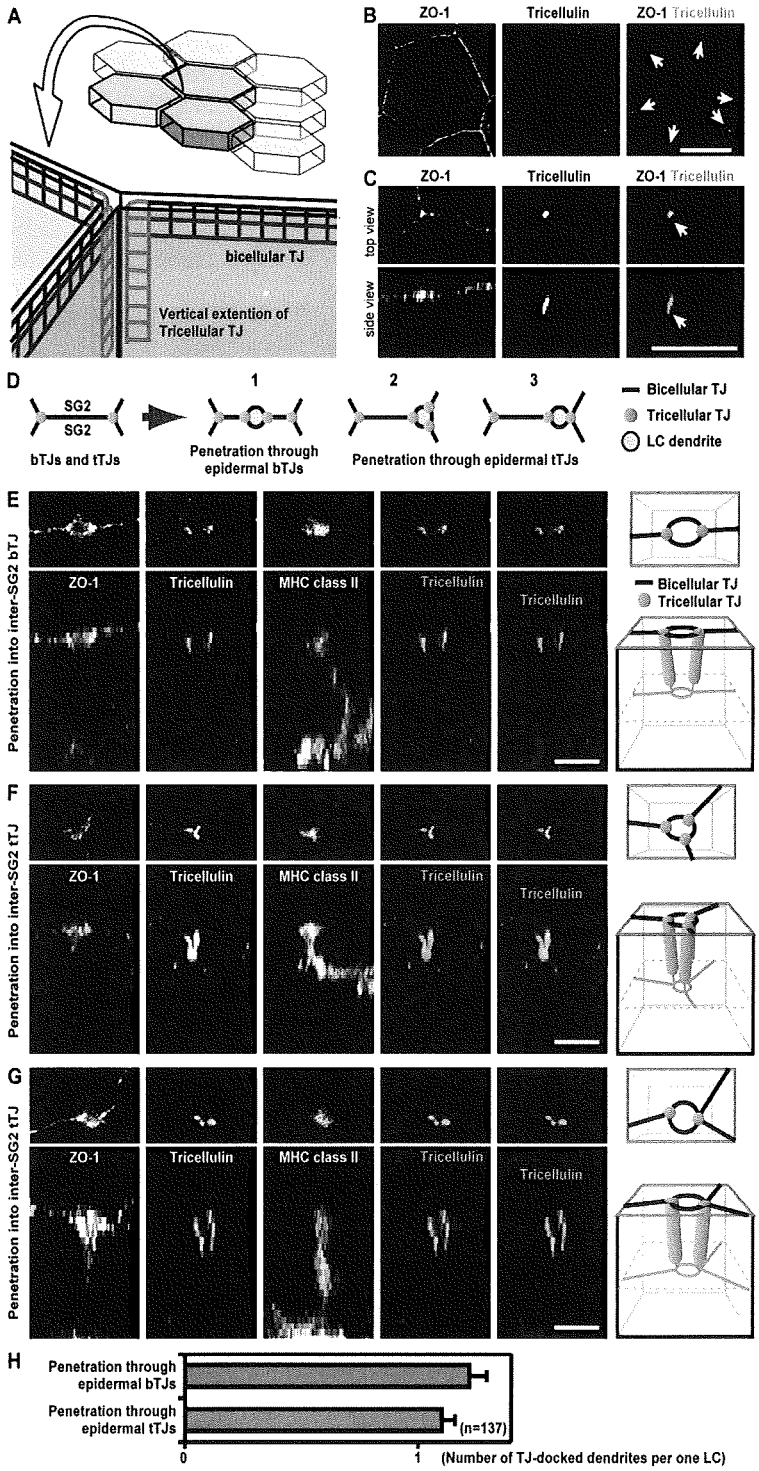

Figure 3. tTJ formation at the TJ penetration point of LC dendrites. (A) Schematic structure of TJs at cell–cell contacts. TJ strands extend vertically below at tricellular contacts to form tTJs (Ikenouchi et al., 2005). (B and C) 3D reconstruction of epidermal sheet stained for ZO-1 and the tTJ protein tricellulin. Tricellulin appears as bright dots (B, arrows) when observed en face, but is found to extend vertically below in 90° rotated images (C, arrows). Bars, 20 µm. (D) Schematic representation of three patterns by which LC dendrites penetrate bTJs or tTJs at the SG2 layer. (E–G) 3D reconstruction images of LC dendrites penetrating TJs as modeled in D (see Video 3). Top rows of each show en face images and bottoms present 90° rotation images accompanied by schematic drawings on the right of each row. Bars, 5 µm. (H) Numbers of bTJ- and tTJ-docked dendrites per LC. The number of dendrites that docked with or penetrated TJs was counted on activated LCs after 12 h of tape stripping. Error bars represent SEM. Data presented in A–G is representative of three mice and data in H of three independent experiments.

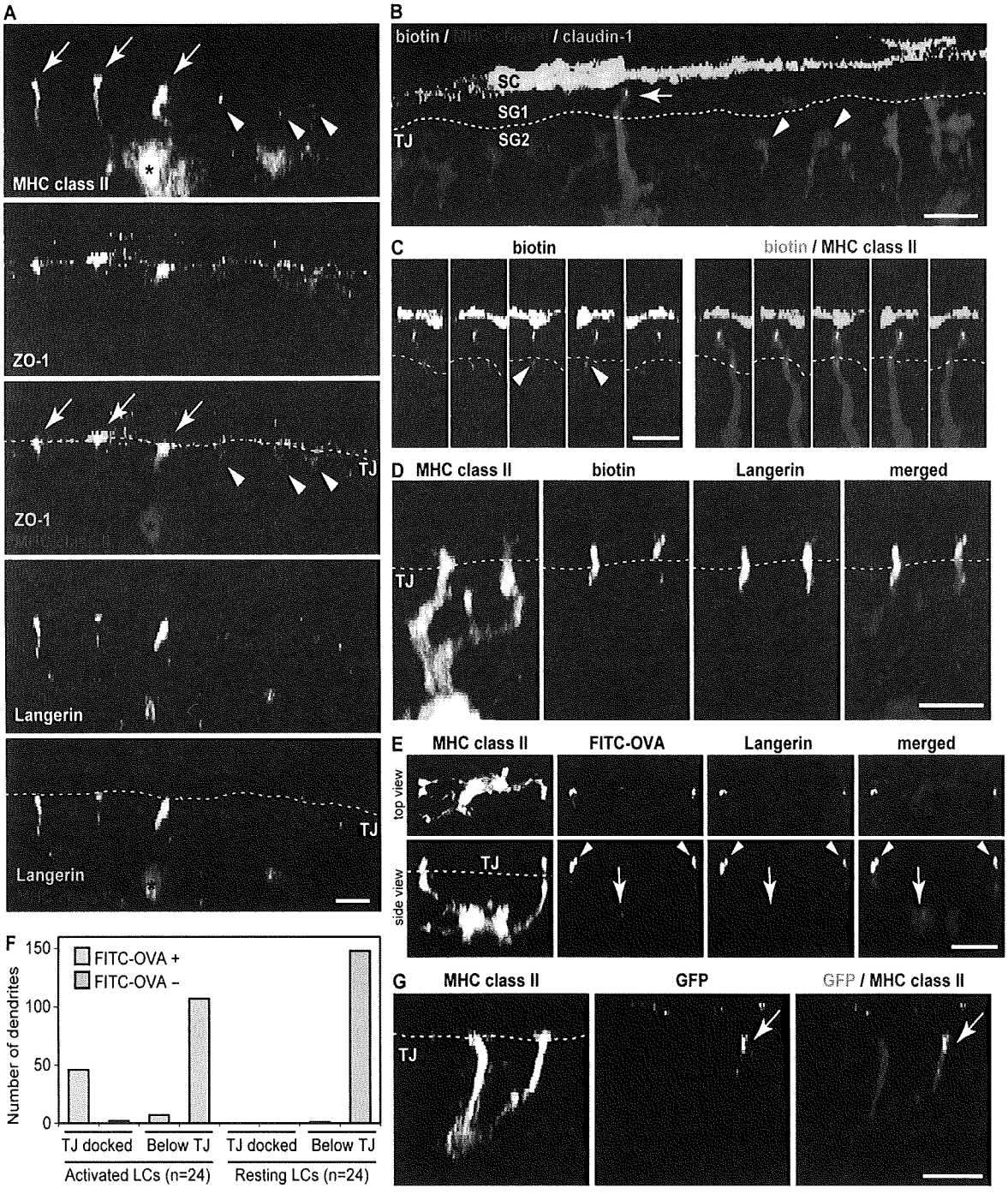

Figure 4. LCs engage in trans-TJ endocytosis via langerin. See Video 4 for more details. (A) Visualization of langerin and MHC II on activated (asterisks) and resting (cell to the right) LCs in relation to TJs as shown by ZO-1 staining. Dashed lines indicate TJs. Langerin accumulated in TJ-docked dendrite tips of activated LCs (arrows). Dendrites of resting LCs (arrowheads) lack langerin accumulation. (B) Biotinylation of LC surface membrane reveals endocytic activity by a TJ-penetrated dendrite (arrow). Dashed lines represent TJs. Dendrites of resting LCs (arrowheads) lack biotin signals. (C) Rotated views of an endocytosing LC dendrite from B. The streak of biotin signal in the dendrite continues within the TJ barrier (arrowheads). (D) Colocalization of biotinylated molecules (green) with langerin (red) in TJ-penetrated dendrites as shown by MHC II (blue) staining. (E) FITC-OVA (green) application demonstrates trans-TJ uptake of Ags by LCs in vivo. FITC-OVA signals colocalized with langerin (red) in TJ-penetrating dendrites (MHC II, blue; arrowheads). Arrows point to accumulation of FITC and langerin signals in perinuclear area of an activated LC. (F) Numbers of FITC-OVA–positive and –negative dendrites. The number of dendrites that docked or did not dock with TJs was counted on resting and activated LCs. (G) GFP-expressing *Escherichia coli* application demonstrates GFP signal within LC dendrite (arrows). Bars, 10 µm. Data presented in A–E and G is representative of three mice and data in F of three independent experiments.

TJ formation between distinct lineages of cells had been poorly described. This study demonstrated that reorganization of epidermal TJ barriers is a dynamic process involving intimate interactions between LCs and the SG2 layer of KCs. This interaction allowed LCs to penetrate their dendrites through TJs, enabling uptake of external Ags in the presence of intact TJ barriers. Tape stripping immediately induced a series of these events and subsequent emigration of activated LCs from the epidermis after 48 h (Fig. S1 A). This indicated that the intraepidermal activation and sequential migration is a well orchestrated biological process for LCs to take up Ags that exist beyond intact TJ barriers without allowing their invasion and, presumably, to present them to the immune system. To our interest, the existence of MHC II–positive intraepidermal DCs has been reported not only in mammals but also in amphibians, reptiles, and birds (Akhter et al., 1993; Pérez-Torres and

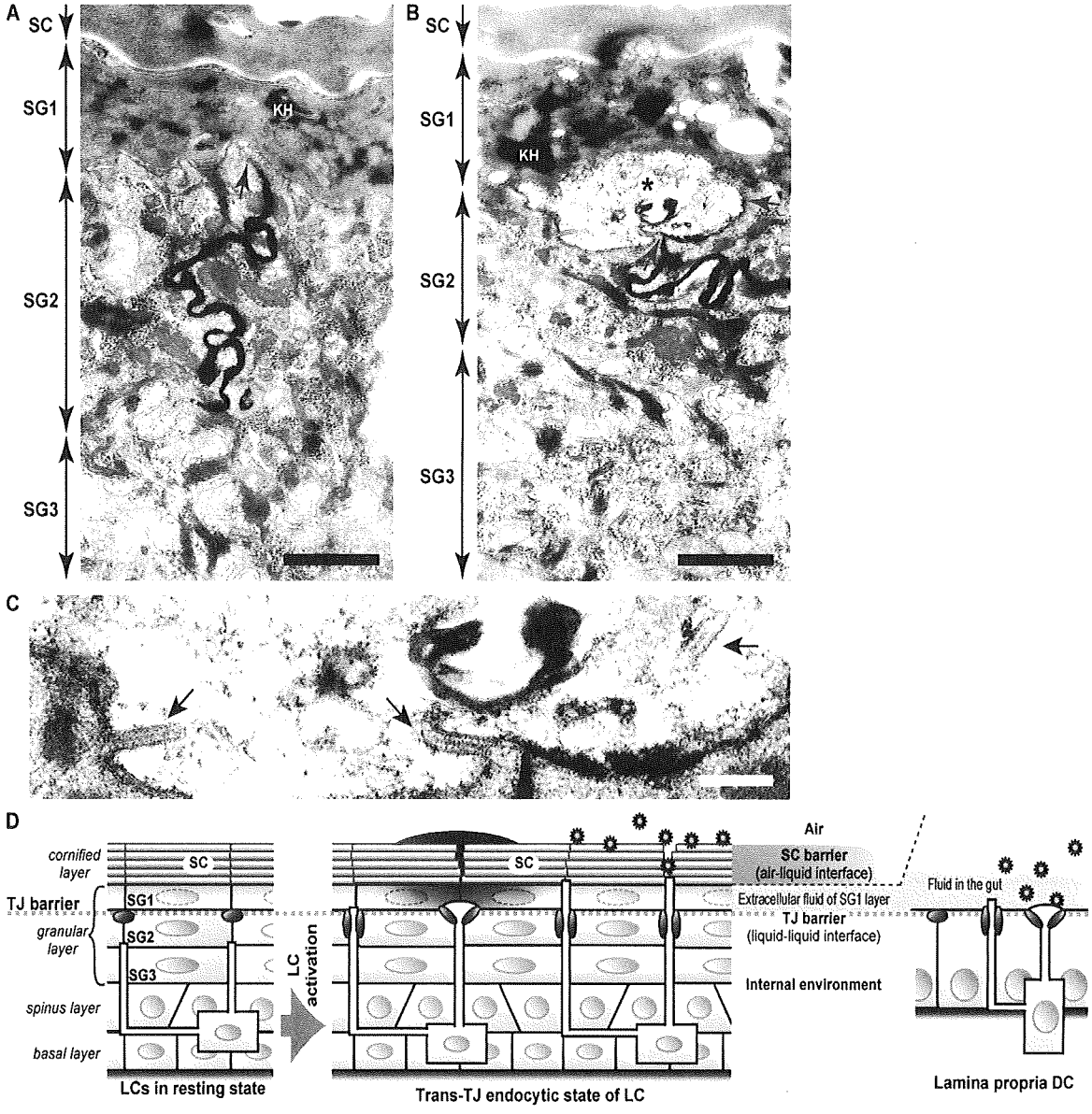

Figure 5. Penetrating dendrites and KCs retain TJ barrier function. Electron microscopy images of SC, SG cells, and dendrite tip of an LC. Keratohyalin granules (KH) identify SG1 cells. (A) Lanthanum permeability assay. Intercellular diffusion of lanthanum nitrate (electron-dense streak) is blocked at KC-KC TJs (arrow). (B) TJ-penetrated LC dendrite (asterisk) was found between the SG1 and SG2 cell layers. The junction between the LC dendrite and SG2 cells also inhibited lanthanum diffusion (arrows), suggesting an intact TJ barrier. Bars, 500 nm. (C) Enlarged image of the LC dendrite tip (B, asterisk), in which two of three Birbeck granules (arrows) were observed to generate from the cell membrane. Bar, 100 nm. (D) Schematic model for trans-TJ uptake activity of LCs. Activation of LCs induces elongation of LC dendrites beyond TJ barriers. bTJs and tTJs that are newly formed between LC and SG2 cells preserve the integrity of TJ barriers during this phenomenon. LCs access Ags that have violated the SC barrier in the presence of intact TJ barrier function. Schematics for gut intraepithelial DCs called lamina propria DCs are shown for comparison. Data presented in A–C is representative of two mice.

Millán-Aldaco, 1994; Pérez-Torres et al., 1995; Castell-Rodríguez et al., 1999). Future study will be needed to clarify that Ag uptake across epidermal TJ barrier by intra-epidermal DCs is an evolutionarily conserved defense system of the skin.

Our findings emphasize the resemblance of the surface barrier system between the epidermis and the gut. In intestinal mucosa, lamina propria DCs have been reported to elongate their dendrites directly into gut lumen to sample bacteria (Rescigno et al., 2001), suggesting that dynamic reorganization of TJs, similar to our finding, occurs between gut DCs and TJs. In comparing these two barrier interfaces, although the surface of the gut epithelial cells that are sealed by TJs is covered by fluid and mucus, which constitutes a liquid–liquid interface system, the surface of epidermis is covered by SC to protect the body from desiccation and coarse microbes or allergens and constitutes an air–liquid interface system (Fig. 5 D). Our findings demonstrate that underneath the SC, but outside the epidermal TJ barriers, is a layer of viable cells called SG1 cells which are likely to be soaked in extracellular fluid. Therefore, similar to the gut, TJs in skin also serve as a liquid–liquid interface barrier. The SG1 layer has never received much focus with regard to barrier function in skin. It appears to be an important layer by not only providing an environment for LCs to take Ags across TJ barriers but also to serve as an intermediate layer that bridges air–liquid and liquid–liquid interfaces (Fig. 5 D).

Our future investigations on the trans-TJ endocytic activity of LCs together with the epidermal barrier system will receive greater focus on the mechanisms or signals that initiate TJ penetration, as well as immunological consequences of this process. This focus should provide new insights not only into pathological conditions such as contact hypersensitivity or chronic atopic dermatitis but should also be of particular interest in the context of antiinfection immunity and percutaneous vaccination.

MATERIALS AND METHODS

Animals. Female C57B6/J 8–12-wk-old mice were used in all experiments. All animal protocols were approved by the animal ethics review board of Keio University and conformed to the National Institutes of Health guidelines.

Immunofluorescence and confocal microscopy. Epidermal sheets were prepared from the ventral side of the mouse ear skin or mouse trunk skin and immunostained as described previously with some modifications (Shelley and Juhlin, 1979; Kubo et al., 2008). Samples were mounted in a whole-mount fashion using Mowiol (EMD) and observed under a fluorescence microscope (BZ-9000; Keyence) equipped with a 20× objective or a laser-scanning confocal microscope (TCS sp5; Leica) equipped with a 63× objective using 0.4–0.5-µm optical slices. 3D reconstruction images were built using sp5 software (Leica). Images and movies were processed using Photoshop CS4 (Adobe), Illustrator CS4 (Adobe), and QuickTime Pro (Apple).

Antibodies. The following antibodies were used in these experiments: anti–claudin-1 polyclonal antibody (pAb; Abcam and Invitrogen), anti–ZO-1 mAb (clone T4-192; Itoh et al., 1991; provided by M. Furuse, Kobe University, Kobe, Japan), anti-tricellulin pAb (Invitrogen), anti-MHC IA/IE mAb (eBioscience), biotinylated anti-MHC IA/IE mAb (eBioscience), Alexa Fluor 488–conjugated anti-GFP pAb (Invitrogen), and anti–mouse Langerin pAb (Imgenex). Species-specific secondary antibodies labeled with Alexa Fluor 488, 568, and 647 (Invitrogen) were used for detection. Biotinylated proteins were detected by Alexa Fluor 568–conjugated streptavidin (Invitrogen), and cell nuclei were stained with Hoechst 33258 (Invitrogen).

LC activation experiments. Ventral sides of mouse ears were used in all experiments. C57BL/6J mice were anaesthetized by intraperitoneal injection of pentobarbital sodium (nembutal; Dainippon Sumitomo Pharma) before LC activation procedures. In tape-stripping experiments, whole-skin surfaces of ventral ears were subsequently tape stripped using scotch tape three times. In cytokine-induced LC activation studies, 50 ng TNF-α (PeproTech) or 50 ng IL-1β (PeproTech) in 30 µl PBS containing 0.7 mM $CaCl_2$ and 0.1% bovine serum albumin (Sigma-Aldrich) or 30 µl of buffer alone was injected subcutaneously into the ventral ear. In topical application experiments, 100 µl of 10 mg/ml EZ-link sulfo-NHS-LC-biotin (Thermo Fisher Scientific) in PBS containing 1 mM $CaCl_2$ was applied to the surface of ventral ear skin. FITC-OVA was delivered by the occlusive dressing technique, in which a small piece of filter paper was moistened by 20 µl PBS or 10 µg FITC-OVA in 20 µl PBS solution and applied to mouse ear skin with Finn chambers (SmartPractice). Finn chambers were covered with adhesive bandages to prevent the mice from scratching them. GFP-expressing *Escherichia coli* was produced by transforming BL21 strain of *Escherichia coli* with pGFP vector (Takara Bio Inc.). GFP-expressing *Escherichia coli* was applied by occlusive dressing technique on ventral ear skin that was tape stripped three times before application. Skin was harvested after the 24-h occlusive application of FITC-OVA or GFP-labeled *Escherichia coli*. It was confirmed that occlusive dressing of PBS alone induced LC activation in situ.

Electron microscopy. Mouse ears were tape stripped 12 h before harvest. Ventral and dorsal sides of the ear were split and the cartilage was removed and fixed with 2.5% glutaraldehyde containing 1% lanthanum nitrate and prepared as described previously (Hashimoto, 1971). Samples were examined with an electron microscope (H-7500; Hitachi High-Technologies) at the accelerating voltage of 80 kV.

Online supplemental material. Fig. S1 shows the time course of LC activation after tape stripping and LC activation induced by subcutaneous injection of TNF-α or IL-1β. Fig. S2 shows TJ docking by activated LCs in mouse trunk skin. Video 1 shows 3D visualization of epidermal structure and TJs in mouse ear skin. Video 2 shows that activated LCs, but not resting LCs, elongate their dendrites and penetrate the TJs. Video 3 shows penetration of LC dendrites through bicellular and tricellular junctions between KCs. Video 4 shows trans-TJ endocytic activity and trans-TJ Ag uptake of LCs. Online supplemental material is available at http://www.jem.org/cgi/content/full/jem.20091527/DC1.

We dedicate this work to the memory of Professor Shoichiro Tsukita.

We thank Drs. Mikio Furuse, Motoyuki Sugai, Stephen I. Katz, John R. Stanley, and Kathleen J. Green for helpful discussions.

This study was partly supported by Grants-in-Aid for Scientific Research, the Promotion of Environmental Improvement for Independence of Young Researchers Project and High-Tech Research Center Project from the Ministry of Education, Culture, Sports, Science and Technology, Japan, and Health Labor Sciences Research Grants for Research on Allergic Diseases and Immunology from the Ministry of Health, Labor and Welfare.

The authors declare no financial conflicts of interest.

Submitted: 15 July 2009
Accepted: 9 November 2009

REFERENCES

Aiba, S., and S.I. Katz. 1990. Phenotypic and functional characteristics of in vivo-activated Langerhans cells. *J. Immunol.* 145:2791–2796.

Akhter, N., M. Kobayashi, and T. Hoshino. 1993. Avian epidermis contains ATPase- and Ia-positive Langerhans-like cells. *Cell Tissue Res.* 271: 103–106. doi:10.1007/BF00297547

Brandner, J.M., S. Kief, C. Grund, M. Rendl, P. Houdek, C. Kuhn, E. Tschachler, W.W. Franke, and I. Moll. 2002. Organization and formation

of the tight junction system in human epidermis and cultured keratinocytes. *Eur. J. Cell Biol.* 81:253–263. doi:10.1078/0171-9335-00244

Castell-Rodríguez, A.E., A. Hernández-Peñaloza, E.A. Sampedro-Carrillo, M.A. Herrera-Enriquez, S.J. Alvarez-Pérez, and A. Rondán-Zarate. 1999. ATPase and MHC class II molecules co-expression in Rana pipiens dendritic cells. *Dev. Comp. Immunol.* 23:473–485. doi:10.1016/S0145-305X(99)00031-2

Enk, A.H., V.L. Angeloni, M.C. Udey, and S.I. Katz. 1993. An essential role for Langerhans cell-derived IL-1 beta in the initiation of primary immune responses in skin. *J. Immunol.* 150:3698–3704.

Farquhar, M.G., and G.E. Palade. 1965. Cell junctions in amphibian skin. *J. Cell Biol.* 26:263–291. doi:10.1083/jcb.26.1.263

Ferreira-Marques, J. 1951. Systema Sensitivum intra epidermicum; the Langerhansian cells as doloriceptores. *Arch Dermatol Syph.* 193:191–249. doi:10.1007/BF00361938

Furuse, M., M. Hata, K. Furuse, Y. Yoshida, A. Haratake, Y. Sugitani, T. Noda, A. Kubo, and S. Tsukita. 2002. Claudin-based tight junctions are crucial for the mammalian epidermal barrier: a lesson from claudin-1–deficient mice. *J. Cell Biol.* 156:1099–1111. doi:10.1083/jcb.200110122

Hashimoto, K. 1971. Intercellular spaces of the human epidermis as demonstrated with lanthanum. *J. Invest. Dermatol.* 57:17–31. doi:10.1111/1523-1747.ep12292052

Ikenouchi, J., M. Furuse, K. Furuse, H. Sasaki, S. Tsukita, and S. Tsukita. 2005. Tricellulin constitutes a novel barrier at tricellular contacts of epithelial cells. *J. Cell Biol.* 171:939–945. doi:10.1083/jcb.200510043

Itoh, M., S. Yonemura, A. Nagafuchi, S. Tsukita, and S. Tsukita. 1991. A 220-kD undercoat-constitutive protein: its specific localization at cadherin-based cell–cell adhesion sites. *J. Cell Biol.* 115:1449–1462. doi:10.1083/jcb.115.5.1449

Kissenpfennig, A., S. Henri, B. Dubois, C. Laplace-Builhé, P. Perrin, N. Romani, C.H. Tripp, P. Douillard, L. Leserman, D. Kaiserlian, et al. 2005. Dynamics and function of Langerhans cells in vivo: dermal dendritic cells colonize lymph node areas distinct from slower migrating Langerhans cells. *Immunity.* 22:643–654. doi:10.1016/j.immuni.2005.04.004

Kubo, A., A. Yuba-Kubo, S. Tsukita, S. Tsukita, and M. Amagai. 2008. Sentan: a novel specific component of the apical structure of vertebrate motile cilia. *Mol. Biol. Cell.* 19:5338–5346. doi:10.1091/mbc.E08-07-0691

Landmann, L., C. Stolinski, and B. Martin. 1981. The permeability barrier in the epidermis of the grass snake during the resting stage of the sloughing cycle. *Cell Tissue Res.* 215:369–382. doi:10.1007/BF00239121

Langerhans, P. 1868. Ueber die Nerven der menschlichen Haut. *Virchows Archiv.* 44:325–337. doi:10.1007/BF01959006

Larsen, C.P., R.M. Steinman, M. Witmer-Pack, D.F. Hankins, P.J. Morris, and J.M. Austyn. 1990. Migration and maturation of Langerhans cells in skin transplants and explants. *J. Exp. Med.* 172:1483–1493. doi:10.1084/jem.172.5.1483

Madison, K.C. 2003. Barrier function of the skin: "la raison d'être" of the epidermis. *J. Invest. Dermatol.* 121:231–241. doi:10.1046/j.1523-1747.2003.12359.x

McGrath, J.A., and J. Uitto. 2008. The filaggrin story: novel insights into skin-barrier function and disease. *Trends Mol. Med.* 14:20–27. doi:10.1016/j.molmed.2007.10.006

Merad, M., F. Ginhoux, and M. Collin. 2008. Origin, homeostasis and function of Langerhans cells and other langerin-expressing dendritic cells. *Nat. Rev. Immunol.* 8:935–947. doi:10.1038/nri2455

Mittal, A.K., and M. Whitear. 1979. Keratinization of fish skin with special reference to the catfish *Bagarius bagarius*. *Cell Tissue Res.* 202:213–230. doi:10.1007/BF00232236

Nagao, K., F. Ginhoux, W.W. Leitner, S. Motegi, C.L. Bennett, B.E. Clausen, M. Merad, and M.C. Udey. 2009. Murine epidermal Langerhans cells and langerin-expressing dermal dendritic cells are unrelated and exhibit distinct functions. *Proc. Natl. Acad. Sci. USA.* 106:3312–3317. doi:10.1073/pnas.0807126106

Niess, J.H., S. Brand, X. Gu, L. Landsman, S. Jung, B.A. McCormick, J.M. Vyas, M. Boes, H.L. Ploegh, J.G. Fox, et al. 2005. CX3CR1-mediated dendritic cell access to the intestinal lumen and bacterial clearance. *Science.* 307:254–258. doi:10.1126/science.1102901

Nishibu, A., B.R. Ward, J.V. Jester, H.L. Ploegh, M. Boes, and A. Takashima. 2006. Behavioral responses of epidermal Langerhans cells in situ to local pathological stimuli. *J. Invest. Dermatol.* 126:787–796. doi:10.1038/sj.jid.5700107

Nishibu, A., B.R. Ward, M. Boes, and A. Takashima. 2007. Roles for IL-1 and TNFalpha in dynamic behavioral responses of Langerhans cells to topical hapten application. *J. Dermatol. Sci.* 45:23–30. doi:10.1016/j.jdermsci.2006.10.003

Oyoshi, M.K., R. He, L. Kumar, J. Yoon, and R.S. Geha. 2009. Cellular and molecular mechanisms in atopic dermatitis. *Adv. Immunol.* 102:135–226. doi:10.1016/S0065-2776(09)01203-6

Pérez Torres, A., and D.A. Millán Aldaco. 1994. Ia antigens are expressed on ATPase-positive dendritic cells in chicken epidermis. *J. Anat.* 184:591–596.

Pérez-Torres, A., D.A. Millán-Aldaco, and A. Rondán-Zárate. 1995. Epidermal Langerhans cells in the terrestrial turtle, *Kinosternum integrum*. *Dev. Comp. Immunol.* 19:225–236. doi:10.1016/0145-305X(95)00006-F

Rescigno, M., M. Urbano, B. Valzasina, M. Francolini, G. Rotta, R. Bonasio, F. Granucci, J.P. Kraehenbuhl, and P. Ricciardi-Castagnoli. 2001. Dendritic cells express tight junction proteins and penetrate gut epithelial monolayers to sample bacteria. *Nat. Immunol.* 2:361–367. doi:10.1038/86373

Shaklai, M., and M. Tavassoli. 1982. Lanthanum as an electron microscopic stain. *J. Histochem. Cytochem.* 30:1325–1330.

Shelley, W.B., and L. Juhlin. 1979. The epidermal helix: a model for the bilayer couple phenomenon. *Arch. Dermatol. Res.* 265:145–152. doi:10.1007/BF00407879

Staehelin, L.A. 1973. Further observations on the fine structure of freeze-cleaved tight junctions. *J. Cell Sci.* 13:763–786.

Streilein, J.W., L.W. Lonsberry, and P.R. Bergstresser. 1982. Depletion of epidermal langerhans cells and Ia immunogenicity from tape-stripped mouse skin. *J. Exp. Med.* 155:863–871. doi:10.1084/jem.155.3.863

Takahara, K., Y. Yashima, Y. Omatsu, H. Yoshida, Y. Kimura, Y.S. Kang, R.M. Steinman, C.G. Park, and K. Inaba. 2004. Functional comparison of the mouse DC-SIGN, SIGNR1, SIGNR3 and Langerin, C-type lectins. *Int. Immunol.* 16:819–829. doi:10.1093/intimm/dxh084

Thomas, W.R., A.J. Edwards, M.C. Watkins, and G.L. Asherson. 1980. Distribution of immunogenic cells after painting with the contact sensitizers fluorescein isothiocyanate and oxazolone. Different sensitizers form immunogenic complexes with different cell populations. *Immunology.* 39:21–27.

Tsukita, S., and M. Furuse. 2002. Claudin-based barrier in simple and stratified cellular sheets. *Curr. Opin. Cell Biol.* 14:531–536. doi:10.1016/S0955-0674(02)00362-9

Tsuruta, D., K.J. Green, S. Getsios, and J.C. Jones. 2002. The barrier function of skin: how to keep a tight lid on water loss. *Trends Cell Biol.* 12:355–357. doi:10.1016/S0962-8924(02)02316-4

Valladeau, J., O. Ravel, C. Dezutter-Dambuyant, K. Moore, M. Kleijmeer, Y. Liu, V. Duvert-Frances, C. Vincent, D. Schmitt, J. Davoust, et al. 2000. Langerin, a novel C-type lectin specific to Langerhans cells, is an endocytic receptor that induces the formation of Birbeck granules. *Immunity.* 12:71–81. doi:10.1016/S1074-7613(00)80160-0

Valladeau, J., C. Dezutter-Dambuyant, and S. Saeland. 2003. Langerin/CD207 sheds light on formation of birbeck granules and their possible function in Langerhans cells. *Immunol. Res.* 28:93–107. doi:10.1385/IR:28:2:93

Wood, L.C., S.M. Jackson, P.M. Elias, C. Grunfeld, and K.R. Feingold. 1992. Cutaneous barrier perturbation stimulates cytokine production in the epidermis of mice. *J. Clin. Invest.* 90:482–487. doi:10.1172/JCI115884

Zimmerli, S.C., and C. Hauser. 2007. Langerhans cells and lymph node dendritic cells express the tight junction component claudin-1. *J. Invest. Dermatol.* 127:2381–2390. doi:10.1038/sj.jid.5700882

The American Journal of Pathology, Vol. 176, No. 5, May 2010

DOI: 10.2353/ajpath.2010.090957

Molecular Pathogenesis of Genetic and Inherited Diseases

Flaky Tail Mouse Denotes Human Atopic Dermatitis in the Steady State and by Topical Application with *Dermatophagoides pteronyssinus* Extract

Catharina Sagita Moniaga,* Gyohei Egawa,*† Hiroshi Kawasaki,‡ Mariko Hara-Chikuma,* Tetsuya Honda,* Hideaki Tanizaki,* Saeko Nakajima,* Atsushi Otsuka,* Hiroyuki Matsuoka,§ Akiharu Kubo,‡ Jun-ichi Sakabe,¶ Yoshiki Tokura,¶ Yoshiki Miyachi,* Masayuki Amagai,‡ and Kenji Kabashima*†

From the Department of Dermatology, and Center for Innovation in Immunoregulative Technology and Therapeutics,† Graduate School of Medicine, Kyoto University, Kyoto; Department of Dermatology,‡ Faculty of Medicine, Keio University, Tokyo; Division of Medical Zoology,§ Jichi Medical University, Tochigi-ken; Department of Dermatology,¶ University of Occupational and Environmental Health, Fukuoka, Japan*

The barrier abnormality, a loss-of-function mutation in the gene encoding filaggrin (*FLG*), which is linked to the incidence of atopic dermatitis (AD), is a recently discovered but important factor in the pathogenesis of AD. Flaky tail (*Flg^{ft}*) mice, essentially deficient in filaggrin, have been used to investigate the role of filaggrin on AD. However, the relevancy of *Flg^{ft}* mice to human AD needs to be determined further. In this study, we observed the clinical manifestations of *Flg^{ft}* mice in the steady state and their cutaneous immune responses against external stimuli, favoring human AD. Under specific pathogen-free conditions, the majority of *Flg^{ft}* mice developed clinical and histological eczematous skin lesions similar to human AD with outside-to-inside skin barrier dysfunction evaluated by newly devised methods. In addition, cutaneous hapten-induced contact hypersensitivity as a model of acquired immune response and a mite extract-induced dermatitis model physiologically relevant to a human AD were enhanced in *Flg^{ft}* mice. These results suggest that the *Flg^{ft}* mouse genotype has potential as an animal model of AD corresponding with filaggrin mutation in human AD. *(Am J Pathol 2010, 176:000–000; DOI: 10.2353/ajpath.2010.090957)*

Atopic dermatitis (AD), which affects at least 15% of children in developed countries, is characterized by eczematous skin lesions, dry skin, and pruritus.[1–3] Although the precise pathogenic mechanism of AD is as yet unknown, several accumulated lines of evidence suggest that a defective skin barrier to environmental stimuli may contribute to its pathogenesis. It has long been thought that the barrier abnormality in AD is not merely an epiphenomenon but rather is the "driver" of disease activity.[4] The evidence for a primary structural abnormality of the stratum corneum in AD is derived from a recently discovered link between the incidence of AD and loss-of-function mutations in the gene encoding filaggrin (*FLG*). Individuals carrying the *FLG* null allele variants tend to develop AD.[5–7]

Filaggrin protein is localized in the granular layers of the epidermis. Profilaggrin, a 400-kDa polyprotein, is the main component of keratohyalin granules.[8–10] In the differentiation of keratinocytes, profilaggrin is dephosphorylated and cleaved into 10 to 12 essentially identical 27-kDa filaggrin molecules, which aggregate in the keratin cytoskeleton system to form a dense protein-lipid matrix.[10] This structure is thought to prevent epidermal water loss and impede the entry of external stimuli, such as allergens, toxic chemicals, and infectious organisms. Therefore, filaggrin is a key protein in the terminal differentiation of the epidermis and in skin barrier function.[11]

Because AD is a common disease for which satisfactory therapies have not yet been established, understanding the mechanism of AD through animal models is an essential issue.[1,12] Flaky tail (*Flg^{ft}*) mice, first introduced in 1958, are spontaneously mutated mice with

Supported in part by the Ministry of Education, Culture, Sports, Science, and Technology of Japan and the Ministry of Health, Labor, and Welfare of Japan.

Accepted for publication January 11, 2010.

Supplemental material for this article can be found on *http://ajp.amjpathol.org*.

Address reprint requests to Dr. Kenji Kabashima, M.D., Ph.D., Department of Dermatology and Center for Innovation in Immunoregulative Technology and Therapeutics, Kyoto University Graduate School of Medicine, 54 Shogoin-Kawara, Kyoto 606-8507, Japan. E-mail: kaba@kuhp.kyoto-u.ac.jp.

abnormally small ears, tail constriction, and a flaky appearance of the tail skin, which is most evident between 5 and 14 days of age.[13] Mice of the *Flg*^{ft} genotype express an abnormal profilaggrin polypeptide that does not form normal keratohyalin F granules and is not proteolytically processed to filaggrin. Therefore, filaggrin is absent from the cornified layers in the epidermis of the *Flg*^{ft} mouse.[14–16]

Recently, it has been revealed that the gene responsible for the characteristic phenotype of *Flg*^{ft} mice is a nonsense mutation of 1-bp deletion analogous tc a common human *FLG* mutation.[15] These mice developed eczematous skin lesions after age 28 weeks under specific pathogen-free (SPF) conditions[17] and enhanced penetration of tracer perfusion determined by ultrastructural visualization,[16] and were predisposed to develop an allergen-specific immune response after epicutaneous sensitization with the foreign allergen ovalbumin (OVA).[15,17] On the other hand, general immunity through intraperitoneal sensitization with OVA was comparable between *Flg*^{ft} mice and control mice.[15,17]

Despite these recent advances, there still remain several issues with *Flg*^{ft} mice to be addressed. For example, serial close observation of clinical manifestations in reference to human AD will be informative. It is of value to evaluate the responses to external stimuli relevant to human AD, such as mite extracts, instead of OVA that has been used previously. A comparative study on the skin-mediated contact hypersensitivity (CHS) response and non-skin-mediated delayed-type hypersensitivity response is important to evaluate the impact of barrier dysfunction on immune responses *in vivo*. In addition, although it has now been determined that the barrier dysfunction is a key element in the establishment of AD, there is no established method to evaluate the outside-to-inside barrier function quantitatively.

In this study, we found that *Flg*^{ft} mice showed spontaneous dermatitis with skin lesions mimicking human AD in a steady state under SPF conditions: serial occurrence of manifestations as scaling, erythema, pruritus, and erosion followed by edema in this order. We also successfully evaluated outside-to-inside barrier dysfunction in *Flg*^{ft} mice quantitatively using a newly developed method. In addition, we determined that the Th1/Tc1-mediated immune response was enhanced by immunization through skin but not through non-skin immunization. Last, we induced severe AD-like skin lesions in *Flg*^{ft} mice by application of mites as a physiologically relevant antigen for human AD, which will be an applicable animal model of AD.

Materials and Methods

Mice

C57BL/6NCrSlc (B6) mice were purchased from SLC (Shizuoka, Japan). Flaky tail (STOCK *a/a ma ft/ma ft*/J; *Flg*^{ft} mice) mice have double-homozygous filaggrin (*Flg*) and matted (*ma*) mutations.[13,14] We used B6 mice as a control of *Flg*^{ft} mice because *Flg*^{ft} mice were described to be outcrossed onto B6 mice at The Jackson Laboratory (Bar Harbor, ME)[13,14] (of note, although the strain was crossed with B6, it is not a B6 congenic strain but rather a hybrid stock that is probably semi-inbred). Female mice were used in all experiments unless otherwise stated; they were maintained on a 12-hour light/dark cycle at a temperature of 24°C and at a humidity of 50 + 10% under SPF conditions at Kyoto University Graduate School of Medicine. Routine colony surveillance and diagnostic workup verified that mice were free of Ectromelia virus, lymphocytic choriomeningitis virus, mouse hepatitis virus, Sendai virus, *Mycoplasma pulmonis*, cilia-associated respiratory bacillus, *Citrobacter rodentium* [*Escherichia coli* O115a,c:K(B)], *Clostridium piliforme* (Tyzzer's organism), *Corynebacterium kutscheri*, *Helicobacter hepaticus*, *Pasteurella pneumotropica*, *Salmonella* spp., parasites, intestinal protozoans, *Enterobius*, and ectoparasites. All experimental procedures were approved by the Institutional Animal Care and Use Committee of Kyoto University Graduate School of Medicine.

Clinical Observation and Histology

The clinical severity of skin lesions was scored according to the macroscopic diagnostic criteria that were used for the NC/Nga mouse.[18] In brief, the total clinical score for skin lesions was designated as the sum of individual scores, graded as 0 (none), 1 (mild), 2 (moderate), and 3 (severe), for the symptoms of pruritus, erythema, edema, erosion, and scaling. Pruritus was observed clinically for more than 2 minutes.

For the histological portion of the study, the dorsal skin of mice was stained with H&E. Toluidine blue staining was used to detect mast cells, and the number of mast cells was calculated as the average from five different fields of each sample ×40 magnification).

Flow Cytometric Analysis and Quantitative RT-PCR

Cells from the skin-draining axillary and inguinal lymph nodes (LNs) and from the spleen were analyzed with flow cytometry. Fluorescent-labeled anti-CD4 and anti-CD8 antibodies were obtained from eBioscience (San Diego, CA) and used to stain cells. The total number of cells per organ and the number of cells in each subset were calculated through flow cytometry using the FACSCanto II system (Becton Dickinson, San Diego, CA). Quantitative RT-PCR was performed as described previously, using the housekeeping gene glyceraldehyde-3-phosphate dehydrogenase (*GAPDH*) as a control.[19]

Total and Mite-Specific Serum IgE

Total serum IgE levels were measured with a mouse IgE ELISA Kit (Bethyl Laboratories, Montgomery, TX) according to the manufacturer's protocols. For the measurement of mite-specific IgE levels, the same type of mouse IgE ELISA Kit was used with slightly modifications. Specifi-

cally, plates were coated and incubated with 10 μg/ml *Dermatophagoides pteronyssinus* (Dp) (Biostir, Kobe, Japan) diluted with coating buffer for 60 minutes. After a blocking period of 30 minutes, 100 μl of 5× diluted serum was added into each well and incubated for 2 hours. Anti-mouse IgE-horseradish peroxidase conjugate (1:15,000; 100 μL) was used to conjugate the antigen-antibody complex for 60 minutes at room temperature; from this point on the ELISA Kit was used according to the manufacturer's protocol. Absorbance was measured at 450 nm. The difference between the sample absorbance and the mean of negative control absorbance was taken as the result.

Skin Barrier Function

The dorsal regions of the skin were shaved in all mice before measurement. To evaluate inside-to-outside barrier function, transepidermal water loss (TEWL) was measured with a Tewameter Vapo Scan (Asahi Biomed, Tokyo, Japan) at 24°C and 46% relative humidity.

Outside-to-inside barrier function was assessed by means of fluorescein isothiocyanate isomer I (FITC) (Sigma-Aldrich, St. Louis, MO). The shaved dorsal skin of mice was treated with 100 μl of 1% FITC diluted in acetone and dibutyl phthalate (1:4); 3 hours later, this area was tape-stripped (Scotch tape, 3M, St. Paul, MN) nine times to remove the stratum corneum containing the remnant of FITC. The painted area (1.2 cm × 1.2 cm) was removed, and FITC concentration was measured. Each skin sample was soaked in PBS at 60°C for 10 seconds, after which the dermis and epidermis were separated. The epidermis was soaked in 500 μl of PBS, homogenized, and spun down at 2200 × *g*. The supernatant was collected, and fluorescence was measured at an excitation wavelength of 535 nm and an emission wavelength of 460 nm using an Arvo SX 1420 counter (Wallac, PerkinElmer, Waltham, MA). The fluorescence value was compared with a standard curve using FITC serial dilutions.

For the evaluation of fluorescence intensities of FITC penetrated into the epidermis, a 1 × 1 cm skin sample was taken after tape stripping, and a 10-μm Tissue-Tek (Sakura Finetek, Tokyo, Japan)-embedded section was analyzed using a BZ-9000 Biorevo digital microscope (Keyence, Osaka, Japan) at the same time exposure.

An *in situ* dye permeability assay with toluidine blue was performed using embryos at 18 days (littermates). Unfixed, untreated embryos were dehydrated by a 1-minute incubation in an ascending series of methanol (25, 50, 74, and 100%) and rehydrated with the descending same methanol series, washed in PBS, and stained with 0.01% toluidine blue.

Scratching Behavior

Scratching behavior was measured in detail using the Sclaba Real system (Noveltec, Kobe, Japan). Mice were put into the machine 20 minutes before measurement to allow them to adapt to the new environment. Ointment was then applied, and the number and duration of scratching sessions were counted according to the manufacturer's protocol for 15 minutes.[20]

Dermatitis Models

For the assessment of irritant contact dermatitis, 20 μl of 0.2 mg/ml phorbol myristate acetate (PMA) (Sigma-Aldrich) was applied to both sides of the ears. Ear thickness change was measured at 1, 3, 12, and 24 hours as well as 5 days after application.

To induce a CHS response, 25 μl of 0.5% 1-fluoro-2.4-dinitrobenzene (DNFB) (Nacalai Tesque, Kyoto, Japan) was painted on the shaved abdomens of mice for sensitization. Five days later, the ears were challenged with 20 μl of 0.2% DNFB, and ear thickness change was measured at 24 and 48 hours after application. Nonsensitized mice were used as a control. A delayed-type hypersensitivity response model was established using OVA (Sigma-Aldrich). Mice were sensitized with 200 μl of 0.5 mg/ml of OVA in complete Freund's adjuvant (Difco Laboratories, Detroit, MI) intraperitoneally and challenged 5 days later with an injection of 20 μl of 1 mg/ml of OVA in incomplete Freund's adjuvant (Difco Laboratories) into the hind footpads. Footpad thickness was measured before and 24 hours after challenge. Nonsensitized mice were used as a control. Footpad swelling was calculated by (footpad thickness change of sensitized mice) − (footpad thickness change of nonsensitized mice). To induce murine AD-like skin lesions, 40 mg of 0.5% Dp in white petrolatum was topically applied to the ears and upper back twice a week for 8 weeks. Petrolatum without Dp was used as a control. One gram of Dp body product (Biostir) contained 1.78 mg of total protein with 2.47 μg of Dp protein (Der p1). Ear thickness and clinical scores were measured every week. Mite-specific IgE levels, TEWL, and histological appearance of eczematous skin were observed 12 hours after the final application.

Statistical Analysis

Data were analyzed using an unpaired two-tailed *t*-test. $P < 0.05$ was considered to be significant.

Results

Spontaneous Dermatitis of Flg^{ft} *Mice in the Steady State under SPF Conditions*

As described previously,[14,15] the expression of the filaggrin monomer was barely detectable by Western blotting in the dorsal skin of *Flg^{ft}* mice compared with that of B6 mice (data not shown). Here, we investigated the clinical manifestations seen in the skin of *Flg^{ft}* mice raised in a steady state under SPF conditions and found that *Flg^{ft}* mice developed spontaneous dermatitis (Figure 1A). The clinical severities of skin lesions, including pruritic activity, erythema, edema, erosion, and scaling, were scored. The total clinical scores of *Flg^{ft}* mice increased with age

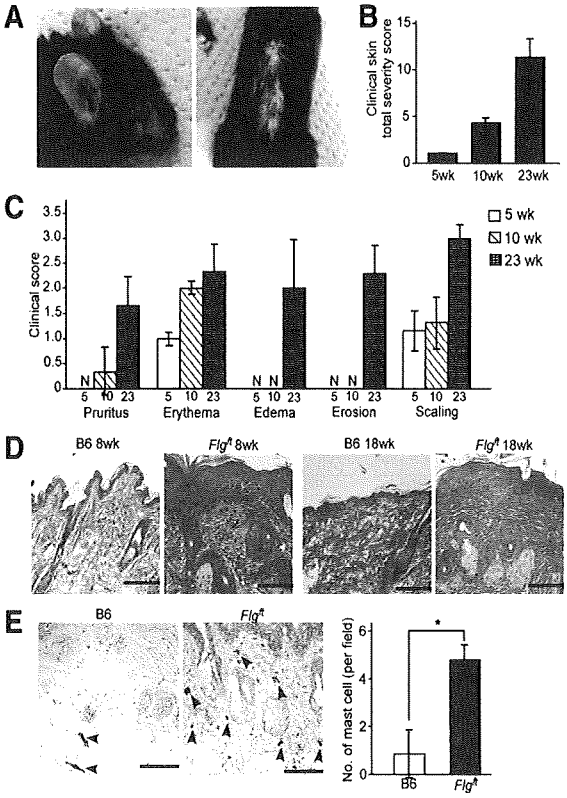

Figure 1. Spontaneous dermatitis in *Flg*^{ft} mice in SPF. **A:** Clinical photographs of 20-week-old *Flg*^{ft} mice. Total clinical severity scores (**B**) for each particular item (**C**) in 5-, 10- and 23-week-old *Flg*^{ft} mice. N, none. **D:** H&E-stained sections in 8- and 18-week-old mice. Scale bar = 100 μm. **E:** Toluidine blue staining of the skin from 8-week-old B6 and *Flg*^{ft} mice and the numbers of mast cells (**arrowheads**) per field are shown. $^*P < 0.05$.

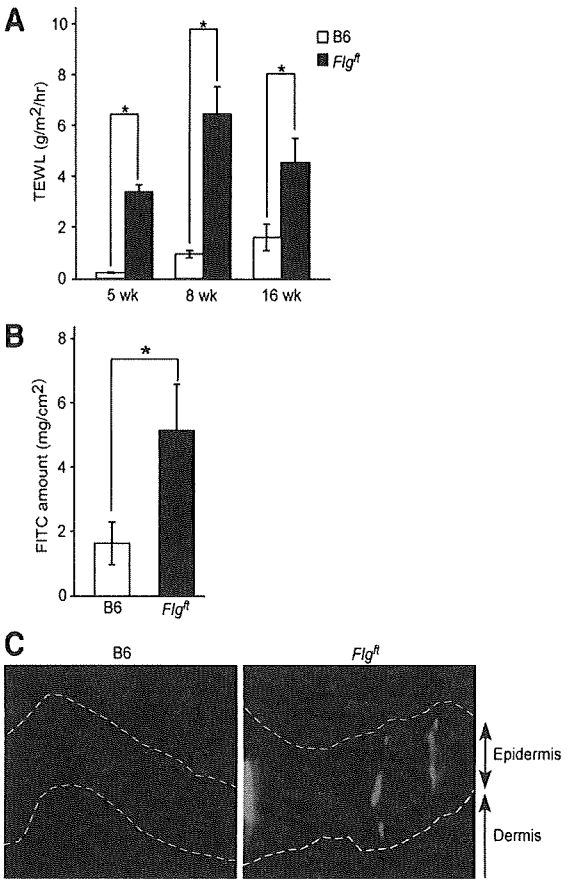

Figure 2. Skin barrier dysfunction in *Flg*^{ft} mice. **A:** TEWL through dorsal skin of 5-, 8-, and 16-week-old B6 and *Flg*^{ft} mice. **B:** Amount of FITC in the skin of B6 and *Flg*^{ft} mice after topical application. **C:** Fluorescence intensities of FITC of the skin after topical application. Dashed white lines indicate the border between the epidermis and the dermis, and the top of the epidermis. $^*P < 0.05$.

(Figure 1B). The first manifestations to appear when mice were young were erythema and fine scaling; pruritic activity, erosion, and edema followed later (Figure 1C). In contrast, no cutaneous manifestation was observed in either B6 mice, studied as a control, or heterozygous mice intercrossed with *Flg*^{ft} and B6 mice kept under SPF conditions throughout the experimental period (data not shown). In addition, there was no apparent difference in terms of clinical manifestations between the genders of *Flg*^{ft} mice throughout the period (data not shown).

Histological examination of skin from *Flg*^{ft} mice revealed epidermal acanthosis, increased lymphocyte infiltration, and dense fibrous bundles in the dermis in both younger (8-week-old) and older (18-week-old) *Flg*^{ft} mice; none of these were observed in B6 mice (Figure 1D). In addition, toluidine blue staining to detect mast cells showed an increased number of mast cells, especially degranulated mast cells in the upper dermis, in *Flg*^{ft} mice (Figure 1E). No mouse or human mite bodies were detected in the sections. These data support the diagnosis of spontaneous clinical dermatitis in *Flg*^{ft} mice in the steady state under SPF conditions.

Defect of Skin Barrier Function in Flg^{ft} *Mice*

Because barrier dysfunction is a common characteristic of AD,[4–7,21] we measured TEWL, an established indicator of barrier function.[21] TEWL was significantly higher in *Flg*^{ft} mice than in B6 mice from an early age (4 weeks) to an older age (16 weeks) (Figure 2A). Because TEWL is only a measure of water transportation through the skin from the inside to the outside of the body, another experimental method was necessary to evaluate outside-to-inside barrier function from the perspective of invasion of external stimuli. To address this issue, we measured FITC penetration through the skin from the outside. FITC solution was applied to the shaved dorsal skin of 8-week-old female mice; 3 hours later, the epidermis was separated and homogenized so that the FITC content could be measured with a fluorometer. The epidermis of *Flg*^{ft} mice contained a higher amount of FITC than that of B6 mice (Figure 2B). Neither group had FITC in the dermis after this procedure, however (data not shown). In addition, observation of fluorescence intensities in the epidermis of both mice showed stronger fluorescence in *Flg*^{ft} mice (Figure 2C). To further analyze the skin permeability, we examined the mouse embryos by toluidine blue solution and showed that the *Flg*^{ft} embryo was entirely dye-permeable compared with the control littermate (Supplemental Figure S1, see *http://ajp.amjpathol.org*). These data strongly indicate a defect in the skin barrier of *Flg*^{ft}

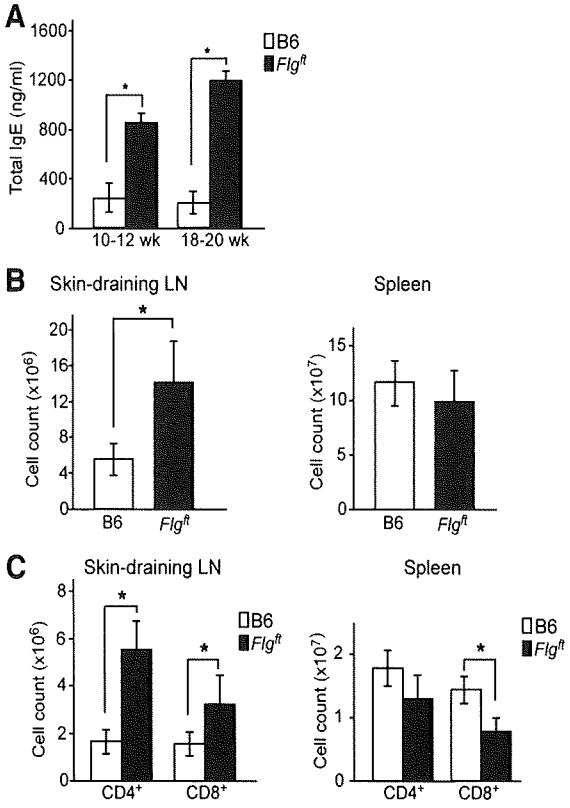

Figure 3. The immune status of *Flg*^{ft} mice in a steady state. **A:** Total serum IgE levels of B6 and *Flg*^{ft} mice as measured by enzyme-linked immunosorbent assay. **B** and **C:** Numbers of total cells (**B**), $CD4^+$ cells, and $CD8^+$ cells in the skin-draining LN and spleen (**C**). $^*P < 0.05$.

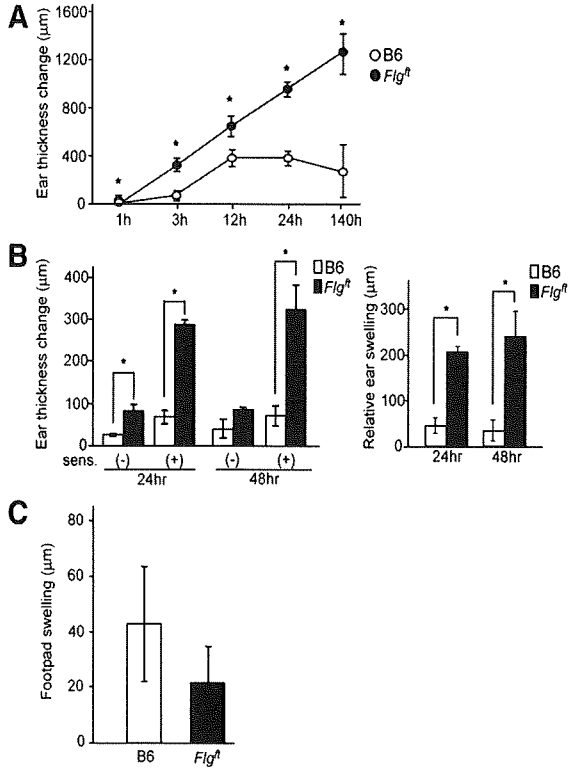

Figure 4. Enhanced cutaneous immune responses in *Flg*^{ft} mice. **A** and **B:** Ear thickness change in B6 and *Flg*^{ft} mice after topical application of PMA as a model of irritant contact dermatitis (**A**), after DNFB challenge on the ears with or without sensitization (**B, left panel**) and the relative ear swelling (**B, right panel**) as a model of CHS. **C:** Delayed-type hypersensitivity response. B6 and *Flg*^{ft} mice were intraperitoneally sensitized with OVA, and challenged through subcutaneous injection to the footpad. Twenty-four hours later, footpad swelling change was measured. $^*P < 0.05$.

mice, both from inside to outside and from outside to inside.

Immune Status in the Steady State

To further elucidate the immune status of *Flg*^{ft} mice in the steady state under SPF conditions, we measured the levels of total serum IgE, because increased severity of AD is known to be correlated with elevated serum IgE levels.[22] IgE levels were significantly higher in *Flg*^{ft} mice than in age-matched B6 mice in the steady state under SPF conditions (Figure 3A). To investigate this matter in greater detail, single cell suspensions from the skin-draining inguinal and axillary LNs and from the spleen were analyzed. The total mononuclear cell number of the LNs was significantly higher in *Flg*^{ft} mice than in B6 mice, but that of the spleen was comparable (Figure 3B). In addition, *Flg*^{ft} mice exhibited significantly higher numbers of $CD4^+$ and $CD8^+$ cells in the skin-draining LNs, but not in the spleen (Figure 3C). Thus, an enhanced immune reaction seems to be induced in *Flg*^{ft} mice by the condition of their skin.

To further analyze the immune condition of the skin, we measured the Th1 (interferon-γ [IFN-γ]), Th2 (interleukin [IL]-4 and IL-13), and Th17 (IL-17) cytokine mRNA levels of dorsal skin of 9-week-old mice in the steady state. The mRNA expression levels of IFN-γ, IL-4, and IL-13 were similar between *Flg*^{ft} and B6 mice, but there was an enhancement in the IL-17 mRNA expression (data not shown) as reported previously.[17]

Enhanced Dermatitis in Flg^{ft} *Mice under External Stimuli*

To characterize the likelihood of various cutaneous immune responses, mice were exposed to various external stimuli. First, we studied the irritant contact dermatitis response to PMA as an irritant agent. When we applied PMA to the ears of B6 and *Flg*^{ft} mice, *Flg*^{ft} mice exhibited an enhanced ear swelling response compared with age-matched B6 mice throughout the experimental period (Figure 4A). Next, we measured the CHS response to DNFB. DNFB was applied to the abdominal skin for sensitization; 5 days later, the ears were challenged with the same hapten. The ear thickness change was more prominent in *Flg*^{ft} mice than in B6 mice (Figure 4B, left panel). On the other hand, the ear thickness change of mice without sensitization was higher for *Flg*^{ft} mice than B6 mice, suggesting that irritation contact dermatitis was enhanced in *Flg*^{ft} mice as expected. To avoid the involvement of this irritation in CHS, we next analyzed the relative ear swelling by subtracting the ear thickness change without sensitization from the ear thickness change with sensitization. The relative ear swelling was more exten-

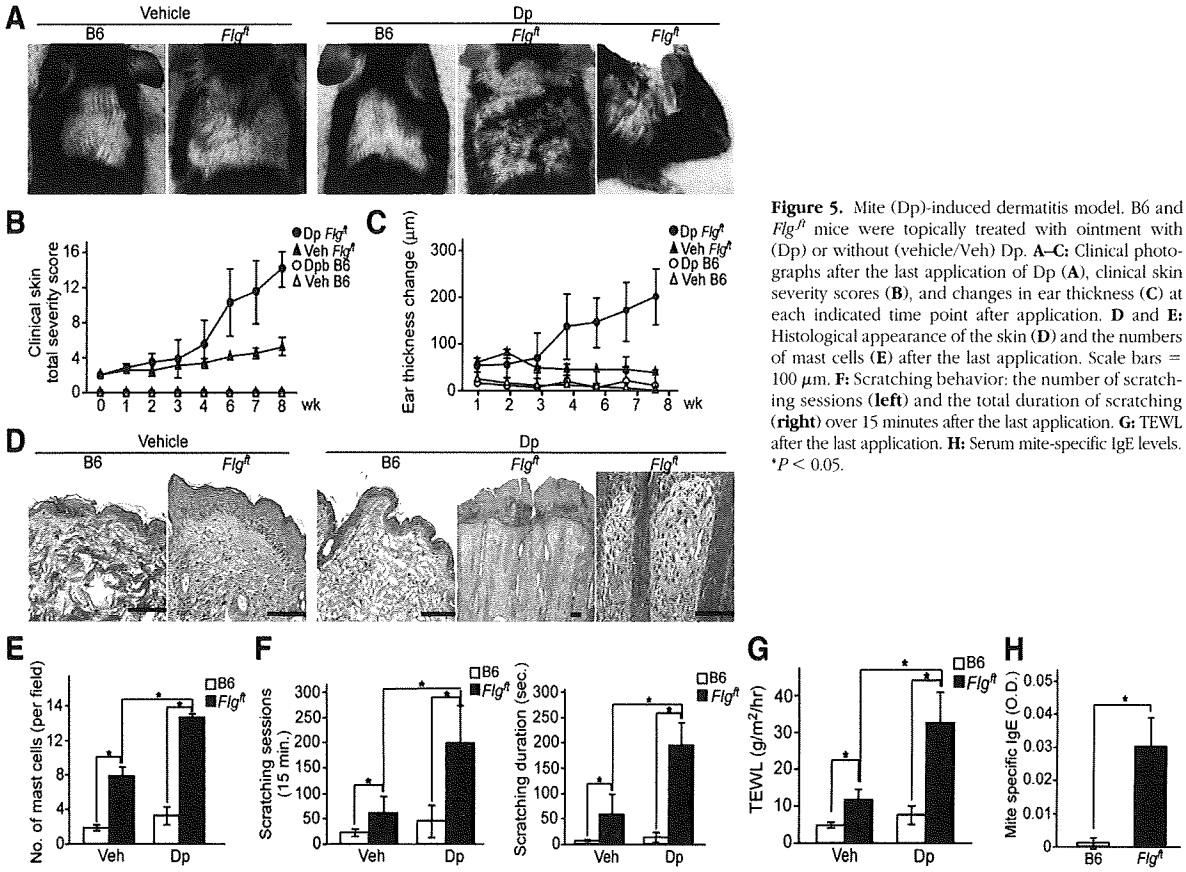

Figure 5. Mite (Dp)-induced dermatitis model. B6 and *Flg*^{ft} mice were topically treated with ointment with (Dp) or without (vehicle/Veh) Dp. **A–C:** Clinical photographs after the last application of Dp (**A**), clinical skin severity scores (**B**), and changes in ear thickness (**C**) at each indicated time point after application. **D** and **E:** Histological appearance of the skin (**D**) and the numbers of mast cells (**E**) after the last application. Scale bars = 100 μm. **F:** Scratching behavior: the number of scratching sessions (**left**) and the total duration of scratching (**right**) over 15 minutes after the last application. **G:** TEWL after the last application. **H:** Serum mite-specific IgE levels. $^{*}P < 0.05$.

sive in *Flg*^{ft} mice than in B6 mice (Figure 4B, right panel). We then measured the relative amount of mRNA for IFN-γ, as a representative Th1 cytokine, to GAPDH as an endogenous control. The relative amount of IFN-γ was higher in the ears of *Flg*^{ft} mice than in those of B6 mice 12 hours after the challenge (0.27 ± 0.13 versus 0.019 ± 0.013, $n = 3$). To further assess the immune responses of *Flg*^{ft} mice, we elicited a delayed-type hypersensitivity response through nonepicutaneous sensitization and challenge. Mice were immunized intraperitoneally with OVA and challenged with a subcutaneous injection of OVA into the footpad. In contrast to the CHS response induced via the skin, the resulting footpad swelling in *Flg*^{ft} mice was lower rather than higher than that in B6 mice (Figure 4C). We also examined the production of mRNA levels of the spleen 3 days after intraperitoneal OVA injection, and it showed a similar level of IFN-γ between *Flg*^{ft} mice and B6 mice (relative mRNA amount to GAPDH: 0.011 ± 0.005 versus 0.016 ± 0.006, $n = 5$). Thus, Th1/Tc1 immune responses were enhanced in *Flg*^{ft} mice only when the stimuli operated via the skin, suggesting that the enhanced immune responses seen in *Flg*^{ft} mice depend on skin barrier dysfunction.

It has been reported that *Flg*^{ft} mice show an enhanced immune response to OVA.[15,17] Their reaction to clinically relevant allergens such as mites has not been evaluated, however. It has also been reported that BALB/c or NC/Nga mice develop an allergic cutaneous immune response to mite antigens when they are applied to the skin after vigorous barrier disruption by means of tape-stripping or SDS treatment.[23,24] Accordingly, we sought to determine whether skin lesions could be induced in *Flg*^{ft} mice through the application of Dp ointment without any skin barrier disruption procedures to evaluate the physiological significance of filaggrin.

The application of Dp ointment to shaved backs and ears induced no cutaneous manifestation in B6 mice throughout the experimental period (Figure 5, A and B), but the same treatment induced dermatitis in *Flg*^{ft} mice, especially on the ears, face, and dorsal skin. Petrolatum alone, used instead of Dp ointment as a control, induced no skin manifestation (Figure 5, A–C). The clinical severity of Dp-induced dermatitis was scored; after 16 applications of Dp ointment over 8 weeks, *Flg*^{ft} mice had developed a very severe skin condition in contrast with the control groups. Consistently, ear swelling in response to Dp ointment was most prominent in *Flg*^{ft} mice (Figure 5C). Histological examination of H&E-stained sections of involved *Flg*^{ft} skin after 16 applications showed acanthosis, elongation of rete ridges, and dense lymphocyte and neutrophil infiltration in the dermis (Figure 5D), accompanied by an increased number of mast cells in the dermis (Figure 5E). We also measured the scratching behavior of *Flg*^{ft} mice treated with Dp using the Sclaba Real system. The number of scratching sessions and the total duration of scratching were significantly higher in *Flg*^{ft} mice than in B6 mice, even among those mice that had not been treated with Dp ointment (Figure 5F); treatment of *Flg*^{ft} mice with Dp ointment raised the number of scratching sessions and the total duration of scratching even higher.

We further evaluated barrier function by measuring TEWL in Dp-treated and untreated mice of each genotype; TEWL was higher in untreated *Flg*^{ft} mice than in B6 mice, and Dp treatment of *Flg*^{ft} mice raised TEWL even higher (Figure 5G). Finally, we examined mite-specific serum IgE levels after the last application and found that *Flg*^{ft} mice had higher levels of Dp-specific IgE than B6 mice had (Figure 5H). Thus, the treatment of *Flg*^{ft} mice with Dp ointment, even without prior barrier disruption, remarkably enhanced both the clinical manifestations and the laboratory findings that correspond to indicators of human AD.

Discussion

Here, we demonstrated that *Flg*^{ft} mice exhibit spontaneous dermatitis with lymphadenopathy, elevated IgE levels, and skin barrier disruption in a steady state under SPF conditions. These outcomes are compatible with the features of human AD, which include chronic eczema, pruritus, and dry skin with elevated TEWL and serum IgE levels.[1–4,25,26] In addition, *Flg*^{ft} mice exhibit enhanced susceptibility to irritant contact dermatitis, CHS, and mite-induced dermatitis compared with B6 mice; these characteristics are also reminiscent of human AD. These results suggest that the barrier defect in this strain of mice leads to spontaneous dermatitis and enhances cutaneous immune responses and inflammation.

Since the first introduction of *Flg*^{ft} mice in 1972,[13] there have been only a few reports of these mice. The first report demonstrated that *Flg*^{ft} mice without the *ma* mutation showed flaky skin as early as postnatal day 2 but became normal in appearance by 3 to 4 weeks of age without spontaneous dermatitis except for their slightly smaller ears.[13] Later, the lack of filaggrin in the epidermis was proposed in the commercially available strain of *Flg*^{ft} mice used in this study, which has both *Flg* and *ma* mutations, as a model of ichthyosis vulgaris, and therefore the cutaneous inflammatory conditions from the perspective of AD was not discussed.[14] There have been three recent studies using *Flg*^{ft} mice as a model of filaggrin deficiency: Fallon et al[15] used *Flg*^{ft} mice from which the *ma* mutation had been eliminated with four additional backcrosses to B6 mice, and others used the commercially available *Flg*^{ft} mice.[16,17] The first report showed only a histological abnormality without clinical manifestations,[15] the second report demonstrated spontaneous eczematous skin lesions after 28 weeks of age,[17] and the third report did not indicate any spontaneous dermatitis in *Flg*^{ft} mice.[16] In our experiment, we observed a spontaneous dermatitis as early as 5 weeks of age with mild erythema and fine scales. These symptoms gradually exacerbated, accompanied by scratching, erosion, and edema, respectively, and became prominent at the age of 23 weeks. The discrepancies among these results seem to be related to the presence or absence of the *ma* mutation and/or variation in the genetic backgrounds of the different strains used and to environmental factors. It has been reported that Japan has higher morbidity for AD than other countries,[27,28] possibly attributable to environmental factors such as pollen.

It has been reported that TEWL, an indicator of inside-to-outside barrier function, is high in both AD patients with the *FLG* mutation[29] and *Flg*^{ft} mice.[15] In consideration of the immunological defense by the skin, however, it is more important to assess outside-to-inside barrier function rather than inside-to-outside barrier function. In fact, outside-to-inside barrier dysfunction has recently been proposed as the most important aspect in the pathogenesis of AD.[9,26] Scharschmidt et al[16] reported increased bidirectional paracellular permeability of water-soluble xenobiotes by ultrastructural visualization in *Flg*^{ft} mice, suggesting a defect of the outside-to-inside barrier. However, the quantitative measurement of this parameter has not been addressed. Here, we propose a new method for evaluating outside-to-inside barrier function quantitatively by measuring the penetrance of FITC through the skin. This method has a parallel correlation with the qualitative measurement of FITC penetrated in epidermis and an established method for skin permeability assay, the *in situ* dye staining method. Therefore, by using this new method, we were able to detect outside-to-inside barrier dysfunction in *Flg*^{ft} mice quantitatively.

The skin abnormality associated with AD is well known to be a predisposing factor to sensitive skin[30,31] and allergic contact dermatitis,[32,33] but patients with AD produce a tuberculin response similar to that of healthy control subjects.[34,35] In humans, sensitive skin is defined as reduced tolerance to cutaneous stimulation, with symptoms ranging from visible signs of irritation to subjective neurosensory discomfort.[30,31] The question of whether human AD patients are more prone to allergic contact dermatitis than nonatopic individuals is still controversial.[33] To address this question, we evaluated skin responsiveness to PMA as an irritant and found that irritant contact dermatitis was enhanced in *Flg*^{ft} mice. In addition, *Flg*^{ft} mice showed an increased skin-sensitized CHS reaction, a form of classic Th1- and Tc1-mediated delayed-type hypersensitivity to haptens, emphasized by increased IFN-γ production. In contrast, when mice were sensitized intraperitoneally, no difference was observed between *Flg*^{ft} and B6 mice *in vivo* or *in vitro*. This finding is consistent with the observation that humans with and without AD respond comparably to tuberculin tests[34,35] and suggests that skin barrier function regulates cutaneous immune conditions, which hints at a possible mechanism involved in human AD.

Clinical studies have provided evidence that a house dust mite allergen plays a causative or exacerbating role in human AD[36] and that a strong correlation exists between patients with *FLG* null alleles and house dust mite-specific IgE.[37] AD-like skin lesions can be induced by repeated topical application of a mite allergen in NC/Nga mice but not in BALB/c mice.[23] In the present study, we induced skin lesions that were clinically and histologically similar to AD, along with increased TEWL, increased scratch behavior, and increased levels of mite-specific IgE, in *Flg*^{ft} mice through the application of Dp. Dp is a common aeroallergen that is frequently involved in induction of human AD. It has protease activities, spe-

cifically from Der p1, Der p3, and Der p9, which may activate protease-activated receptor-2 in human keratinocytes.[38,39] A recent report has shown that activation of protease-activated receptor-2 through Dp application significantly delays barrier recovery rate in barrier function-perturbed skin or compromised skin.[39] Therefore, Dp may play a dual role in the onset of AD, both as an allergen and proteolytic signal and as a perturbation factor of the barrier function, leading to the persistence of eczematous skin lesions in AD.[39,40]

To address the issue of variable genetic background, we observed immune responses in mice of other genotypes, such as BALB/c and C3H, as controls, but both of these lines exhibited much less severe CHS responses compared with those in *Flg*^{ft} mice (data not shown), suggesting that the enhanced immune responses seen in *Flg*^{ft} mice were not solely due to their genetic background. The effect of the *ma* mutation in relation to the *ft* mutation in commercially available *Flg*^{ft} mice in the development of AD-like skin lesions needs to be clarified in future studies. Furthermore, our study showed that heterozygous mice intercrossed with *Flg*^{ft} mice and B6 mice did not develop spontaneous dermatitis. In this way they are unlike human AD patients, most of whom are heterozygous for the *FLG* mutation. Not only human studies but also additional mouse studies are required to clarify these relationships.

In this study, we have shown that *Flg*^{ft} mice exhibit spontaneous dermatitis resembling human AD, enhanced irritation dermatitis and a contact hypersensitivity response, and mite-induced AD-like skin lesions, which provide hints for possible mechanisms in the human disease. These results suggest that *Flg*^{ft} mice have the potential to serve as an animal model of human AD and further accentuate the important role of filaggrin in skin barrier function in the pathogenesis of AD.

References

1. Jin H, He R, Oyoshi M, Geha RS: Animal models of atopic dermatitis. J Invest Dermatol 2009, 129:31–40
2. Wollenberg A, Bieber T: Atopic dermatitis: from the genes to skin lesions. Allergy 2000, 55:205–213
3. Novak N, Bieber T, Leung DY: Immune mechanism leading to atopic dermatitis. J Allergy Clin Immunol 2003, 112:S128–S139
4. Elias PM, Hatano Y, Williams ML: Basis for the barrier abnormality in atopic dermatitis: outside-inside-outside pathogenic mechanism. J Allergy Clin Immunol 2008, 121:1337–1343
5. Palmer CN, Irvine AD, Terron-Kwiatkowski A, Zhao Y, Liao H, Lee SP, Goudie DR, Sandilands A, Campbell LE, Smith FJ, O'Regan GM, Watson RM, Cecil JE, Bale SJ, Compton JG, DiGiovanna JJ, Fleckman P, Lewis-Jones S, Arseculeratne G, Sergeant A, Munro CS, El Houate B, McElreavey K, Halkjaer LB, Bisgaard H, Mukhopadhyay S, McLean WH: Common loss-of function variants of the epidermal barrier protein filaggrin are a major predisposing factor for atopic dermatitis. Nat Genet 2006, 38:441–446
6. Nomura T, Sandilands A, Akiyama M, Liao H, Evans AT, Sakai K, Ota M, Sugiura H, Yamamoto K, Sato H, Palmer CN, Smith FJ, McLean WH, Shimizu H: Unique mutations in the filaggrin gene in Japanese patients with ichthyosis vulgaris and atopic dermatitis. J Allergy Clin Immunol 2007, 119:434–440
7. Morar N, Cookson WO, Harper JI, Moffat MF: Filaggrin mutations in children with severe atopic dermatitis. J Invest Dermatol 2007, 127:1667–1672
8. Dale BA: Filaggrin, the matrix protein of keratin. Am J Dermatopathol 1985, 7:65–68
9. Listwan P, Rothnagel JA: Keratin bundling proteins. Methods Cell Biol 2004, 78:817–827
10. Candi E, Schmidt R, Melino G: The cornified envelope: a model of cell death in the skin. Nat Rev Mol Cell Biol 2005, 6:328–340
11. Gan SQ, McBride OW, Idler WW, Markova N, Steinert RM: Organization, structure, and polymorphisms of the human profilaggrin gene. Biochemistry 1990, 29:9432–9440
12. Shiohara T, Hayakawa J, Mizukawa Y: Animal models for atopic dermatitis: are they relevant to human disease? J Dermatol Sci 2004, 36:1–9
13. Lane P: Two new mutations in linkage group XVI of the house mouse. J Hered 1972, 63:135–140
14. Presland RB, Boggess D, Lewis SP, Hull C, Fleckman P, Sundberg JP: Loss of normal profilaggrin and filaggrin in flaky tail (*ft/ft*) mice: an animal model for the filaggrin-deficient skin disease ichthyosis vulgaris. J Invest Dermatol 2000, 115:1072–1081
15. Fallon PG, Sasaki T, Sandilands A, Campbell LE, Saunders SP, Mangan NE, Callanan JJ, Kawasaki H, Shiohama A, Kubo A, Sundberg JP, Presland RB, Fleckman P, Shimizu N, Kudoh J, Irvine AD, Amagai M, McLean WH: A homozygous frameshift mutation in the mouse *Flg* gene facilitates enhanced percutaneous allergen priming. Nat Genet 2009, 41:602–608
16. Scharschmidt TC, Man MQ, Hatano Y, Crumrine D, Gunathilake R, Sundberg JP, Silva KA, Mauro TM, Hupe M, Cho S, Wu Y, Celli A, Schmuth M, Feingold KR, Elias PM: Filaggrin deficiency confers a paracellular barrier abnormality that reduces inflammatory thresholds to irritants and haptens. J Allergy Clin Immunol 2009, 124:496–506, 506.e1–e6
17. Oyoshi MK, Murphy GF, Geha RS: Filaggrin-deficient mice exhibit Th17-dominated skin inflammation and permissiveness to epicutaneous sensitization with protein antigen. J Allergy Clin Immunol 2009, 124:475–493, 493.e1
18. Leung DY, Hirsch RL, Schneider L, Moody C, Takaoka R, Li SH, Meyerson LA, Mariam SG, Goldstein G, Hanifin JM: Thymopentin therapy reduces the clinical severity of atopic dermatitis. J Allergy Clin Immunol 1990, 85:927–933
19. Mori T, Kabashima K, Yoshiki R, Sugita K, Shiraishi N, Onoue A, Kuroda E, Kobayashi M, Yamashita U, Tokura Y: Cutaneous hypersensitivities to hapten are controlled by IFN-γ-upregulated keratinocyte Th1 chemokines and IFN-γ-downregulated Langerhans cell Th2 chemokines. J Invest Dermatol 2008, 128:1719–1727
20. Orito K, Chida Y, Fujisawa C, Arkwright PD, Matsuda H: A new analytical system for quantification scratching behavior in mice. Br J Dermatol 2004, 150:33–38
21. Gupta J, Grube E, Ericksen MB, Stevenson MD, Lucky AW, Sheth AP, Assa'ad AH, Khurana Hershey GK: Intrinsically defective skin barrier function in children with atopic dermatitis correlates with disease severity. J Allergy Clin Immunol 2008, 121:725–730
22. Novak N: New insights into the mechanism and management of allergic diseases: atopic dermatitis. Allergy 2009, 64:265–275
23. Kang JS, Lee K, Han SB, Ahn JM, Lee H, Han MH, Yoon YD, Yoon WK, Park SK, Kim HM: Induction of atopic eczema/dermatitis syndrome-like skin lesions by repeated topical application of a crude extract of Dermatophagoides pteronyssinus in NC/Nga mice. Int Immunopharmacol 2006, 6:1616–1622
24. Yamamoto M, Haruna T, Yasui K, Takahashi H, Iduhara M, Takaki S, Deguchi M, Arimura A: A novel atopic dermatitis model induced by topical application with *Dermatophagoides farinae* extract in NC/Nga mice. Allergol Int 2007, 56:139–148
25. Matsumoto M, Ra C, Kawamoto K, Sato H, Itakura A, Sawada J, Ushio H, Suto H, Mitsuishi K, Hikasa Y, Matsuda H: IgE hyperproduction through enhanced tyrosine phosphorylation of Janus kinase 3 in NC/Nga mice, a model for human atopic dermatitis. J Immunol 1999, 162:1056–1063
26. Cooper D, Hales J, Camp R: IgE-dependent activation of T cells by allergen in atopic dermatitis: pathophysiologic relevance. J Invest Dermatol 2004, 123:1086–1091
27. The International Study of Asthma and Allergies in Childhood (ISAAC) Steering Committee: Worldwide variation in prevalence of symptoms of asthma, allergic rhinoconjunctivitis, and atopic eczema: ISAAC. Lancet 1998, 351:1225–1232
28. Williams H, Robertson C, Stewart A, Aït-Khaled N, Anabwani G,

Anderson R, Asher I, Beasley R, Björkstén B, Burr M, Clayton T, Crane J, Ellwood P, Keil U, Lai C, Mallol J, Martinez F, Mitchell E, Montefort S, Pearce N, Shah J, Sibbald B, Strachan D, von Mutius E, Weiland S: Worldwide variations in the prevalence of symptoms of atopic eczema in the international study of asthma and allergies in childhood. J Allergy Clin Immunol 1999, 103:125–138

29. Nemoto-Hasebe I, Akiyama M, Nomura T, Sandilands A, McLean WHI, Shimizu H: Clinical severity correlates with impaired barrier in filaggrin-related eczema. J Invest Dermatol 2009, 129:682–689
30. Willis CM, Shaw S, De Lacharrière O, Baverel M, Reiche L, Jourdain R, Bastien P, Wilkinson JD: Sensitive skin: an epidemiological study. Br J Dermatol 2001, 145:258–263
31. Farage MA, Katsarou A, Maibach HI: Sensory, clinical and physiological factors in sensitive skin: a review. Contact Dermatitis 2006, 55:1–14
32. Clayton TH, Wilkinson SM, Rawcliffe C, Pollock B, Clark SM: Allergic contact dermatitis in children: should pattern of dermatitis determine referral? A retrospective study of 500 children tested between 1995 and 2004 in one UK centre. Br J Dermatol 2006, 154:114–117
33. Mailhol C, Lauwers-Cances V, Rance F, Paul C, Giordano-Labadie F: Prevalence and risk factors for allergic contact dermatitis to topical treatment in atopic dermatitis: a study in 641 children. Allergy 2009, 64:801–806
34. Yilmaz M, Bingöl G, Altintas D, Kendirli SG: Correlation between atopic diseases and tuberculin responses. Allergy 2000, 55:664–667
35. Grüber C, Kulig M, Bergmann R, Guggenmoos-Holzmann I, Wahn U, MAS-90 Study Group: Delayed hypersensitivity to tuberculin, total immunoglobulin E, specific sensitization, and atopic manifestation in longitudinally followed early Bacille Calmette-Guèrin-vaccinated and nonvaccinated children. Pediatrics 2001, 107:e36
36. Kimura M, Tsuruta S, Yoshida T: Correlation of house dust mite-specific lymphocyte proliferation with IL-5 production, eosinophilia, and the severity of symptoms in infants with atopic dermatitis. J Allergy Clin Immunol 1998, 101:85–89
37. Henderson J, Northstone K, Lee SP, Liao H, Zhao Y, Pembrey M, Mukhopadhyay S, Smith GD, Palmer CN, McLean WH, Irvine AD: The burden of disease associated with filaggrin mutations: a population-based, longitudinal birth cohort study. J Allergy Clin Immunol 2008, 121:872–877
38. Vasilopoulos Y, Cork MJ, Teare D, Marinou I, Ward SJ, Duff GW, Tazi-Ahnini R: A nonsynonymous substitution of cystatin A, a cysteine protease inhibitor of house dust mite protease, leads to decreased mRNA stability and shows a significant association with atopic dermatitis. Allergy 2007, 62:514–519
39. Jeong SK, Kim HJ, Youm JK, Ahn SK, Choi EH, Sohn MH, Kim KE, Hong JH, Shin DM, Lee SH: Mite and cockroach allergens activate protease-activated receptor 2 and delay epidermal permeability barrier recovery. J Invest Dermatol 2008, 128:1930–1939
40. Roelandt T, Heughebaert C, Hachem JP: Proteolytically active allergens cause barrier breakdown. J Invest Dermatol 2008, 128:1878–1880